Environmental Pollution 286 (2021) 117317

Contents lists available at ScienceDirect

Environmental Pollution

journal homepage: www.elsevier.com/locate/envpol

Source identification of atmospheric particle-bound mercury in the Himalayan foothills through non-isotopic and isotope analyses☆

Junming Guo [a], Chhatra Mani Sharma [a,b], Lekhendra Tripathee [a,c,*], Shichang Kang [a,d,e], Xuewu Fu [f], Jie Huang [g], Kundan Lal Shrestha [h], Pengfei Chen [a]

[a] State Key Laboratory of Cryospheric Science, Northwest Institute of Eco-environment and Resources, Chinese Academy of Sciences (CAS), Lanzhou, 730000, China
[b] Central Department of Environmental Science, Tribhuvan University, Kathmandu, Nepal
[c] Himalayan Environment Research Institute (HERI), Kathmandu, Nepal
[d] CAS Center for Excellence in Tibetan Plateau Earth Sciences, Beijing, 100085, China
[e] University of Chinese Academy of Sciences, Beijing, 100049, China
[f] State Key Laboratory of Environmental Geochemistry, Institute of Geochemistry, Chinese Academy of Sciences, 99 Lincheng West Road, Guiyang, 550081, China
[g] Key Laboratory of Tibetan Environment Changes and Land Surface Processes, Institute of Tibetan Plateau Research, Chinese, Academy of Sciences, Beijing, 100101, China
[h] Department of Environmental Science and Engineering, Kathmandu University, Dhulikhel, Nepal

ARTICLE INFO

Keywords:
Particle-bound mercury (HgP)
Stable mercury isotopes
Aerosols
South Asia

ABSTRACT

This study reports on the sources of atmospheric particle-bound mercury (HgP) in less studied regions of Nepal based on the analysis of stable mercury (Hg) isotopes in aerosol samples from two neighboring areas with high and low anthropogenic emissions (Kathmandu and Dhulikhel, respectively) during 2018. Although the Indian monsoon and westerlies are generally regarded as the primary carriers of pollutants to this region via the heavily industrialized Indo-Gangetic Plain, the concentrations of total suspended particles (TSP) and HgP in Kathmandu were higher than those in Dhulikhel, thus suggesting a substantial contribution from local sources. Both isotopic (δ^{200}Hg and Δ^{199}Hg) and non-isotopic evidence indicated that dust, waste burning, and industrial byproducts (without Hg amalgamation) were the major sources of Hg in Kathmandu during the study period. Mercury may have been transported via air masses from Kathmandu to Dhulikhel, as indicated by the similar organic carbon/elemental carbon ratios and seasonal trends of TSP and HgP in these two locations. Local anthropogenic sources were found to contribute significantly to atmospheric Hg pollution through dust resuspension. Therefore, dust resuspension should be considered when evaluating the long-range transport of air pollutants such as Hg, particularly in anthropogenically stressed areas.

1. Introduction

Through long-range transport, mercury (Hg) is readily deposited on glaciers and in aquatic and terrestrial ecosystems in remote, pristine environments (Lindberg et al., 2007; Obrist et al., 2011; Qie et al., 2018; Tripathee et al., 2019b). Studies have indicated both natural and anthropogenic sources of Hg emissions (Fang et al., 2016; Schleicher et al., 2015; Tang et al., 2019; Xu et al., 2015). The three main forms of atmospheric Hg are gaseous elemental Hg, particle-bound Hg (HgP), and gaseous oxidized Hg (GOM), which account for more than 95% of the total atmospheric Hg (Cheng et al., 2017; Kim et al., 2012; Li et al., 2017). Particle-bound Hg contributes crucially to the deposition process (Tang et al., 2019) and, as a potential neurotoxin, constitutes a direct public health concern.

South Asia is becoming a Hg pollution hotspot because of rapid economic growth and industrialization (Burger Chakraborty et al., 2013; Huang et al., 2020b; Mukherjee et al., 2009). Stable Hg isotopes have become a useful proxy for the identification of Hg sources (Fu et al., 2019; Huang et al., 2016; Sun et al., 2016; Yuan et al., 2020), particularly as a result of improvements in high-precision analytical methods (Blum and Johnson, 2017; Yamakawa et al., 2020). Two Hg fractionation mechanisms are used for source identification and biogeochemical

☆ This paper has been recommended for acceptance by Admir C. Targino.

* Corresponding author. State Key Laboratory of Cryospheric Science, Northwest Institute of Eco-environment and Resources, Chinese Academy of Sciences (CAS), Lanzhou, 730000, China.
E-mail address: lekhendra.t@gmail.com (L. Tripathee).

https://doi.org/10.1016/j.envpol.2021.117317
Received 29 December 2020; Received in revised form 30 April 2021; Accepted 3 May 2021
Available online 6 May 2021

analysis (Bergquist and Blum, 2007; Blum et al., 2014; Kwon et al., 2020; Sonke, 2011): mass-independent fractionation (Hg-MIF; Δ^{199}Hg) and mass-dependent fractionation (Hg-MDF; δ^{202}Hg).

Several studies undertaken in North America and Europe have focused on the spatiotemporal distribution of HgP and reported atmospheric Hg levels that were lower than those in urban areas (Gratz et al., 2013; Li et al., 2008; Siudek et al., 2016; Song et al., 2009). Numerous studies conducted in East Asian countries, such as China (Han et al., 2018; Schleicher et al., 2016; Tang et al., 2019; Yu et al., 2016; Zhu et al., 2014), Japan (Sakata and Marumoto, 2002), and South Korea (Nguyen et al., 2016) have attributed relatively high HgP concentrations to primary sources including coal burning and metal smelting (Fu et al., 2011). Limited data are available on the stable isotopes of Hg or their application in source apportionment in South Asia. Furthermore, only a few studies in the Indian territories have considered Hg pollution through isotopic analysis (Das et al., 2016), and to the best of our knowledge, no such investigations have been undertaken in the Nepalese Himalayas (the highest mountain range in the world). A 2020 study of Lake Gokyo sediments found no relationship between Hg and organic carbon (OC), and it was considered that most of the Hg was transported to remote high-altitude areas of the Nepalese Himalayas by the South Indian monsoon (Huang et al., 2020b). Therefore, studies on atmospheric Hg are important for understanding the atmospheric concentrations, sources, transport mechanisms, and fate of HgP in the Himalayan foothills. Moreover, the use of stable isotopes to investigate the major sources and environmental impacts of anthropogenic Hg pollution in the Himalayas may facilitate improvements in the assessment and mitigation of anthropogenic pollution.

Natural organic matter in tropical forest soils plays a crucial role in the transformation of Hg through dark reduction (Yuan et al., 2020). Therefore, elucidating the relationship between HgP and carbonaceous particles organic carbon (OC) and elemental carbon (EC) may extend our understanding of the transport of Hg through the atmosphere.

To examine the levels, seasonality, and sources of HgP in the Himalayan atmosphere, aerosol samples were collected from rural and urban sites (Dhulikhel and Kathmandu, respectively) within the Atmospheric Pollution and Cryospheric Change observation network (Kang et al., 2019). Furthermore, this study evaluated the resuspension of Hg in the urban Kathmandu Valley. Simultaneous sampling of stable Hg isotopes was performed in the Kathmandu Valley, urban area, and in Dhulikhel, a downwind rural area located 30 km to the southeast of the Kathmandu Valley. The findings of this study are expected to yield new insights into the local, regional, and long-range transport pathways of HgP in South Asia.

2. Materials and methods

2.1. Study area and sampling procedures

Hence, aerosol samples (n = 72) were collected from Kathmandu University in Dhulikhel (27.6196° N and 85.5386° E, 1514 m above sea level; Fig. 1) from January to December 2018 (i.e., 1 year). A total suspended particulate (TSP) sampler was placed on the rooftop of the university library building, which is bounded by playgrounds and an agricultural field to the east, west, and north, and a few residential buildings to the south. We collected TSP and fine particulate matter ($PM_{2.5}$, aerodynamic diameter of <2.5 μm) samples (n = 24) during the pre-monsoon period (March–May 2018) from an urban residential area in the Kathmandu Valley (27.69° N, 85.4 0° E, approximately 1300 m above sea level). Simultaneous TSP sampling (n = 13) was performed in Dhulikhel and Kathmandu. The major sources of air pollutants in the Kathmandu Valley are dust and anthropogenic emissions from vehicles, brick kilns, waste burning, and factories (Guo et al., 2017; Tripathee et al., 2017). Brick kilns that use low-quality coal in the valley are active during the dry season (October–May), but not during the monsoon season (June–September). In contrast, there are negligible pollution sources in Dhulikhel. However, pollutants are carried by local winds from the Kathmandu Valley and through long-distance transport from the Indo-Gangetic Plain (IGP) region and West Asia, especially during the dry season.

2.2. Collection of atmospheric HgP samples

For the sampling of TSP and $PM_{2.5}$, pre-weighed quartz fiber filters (QM-A, diameter of 90 mm; Whatman, Maidstone, UK) were preheated at 500 °C for 6 h and placed in a medium-volume sampler (T2034,

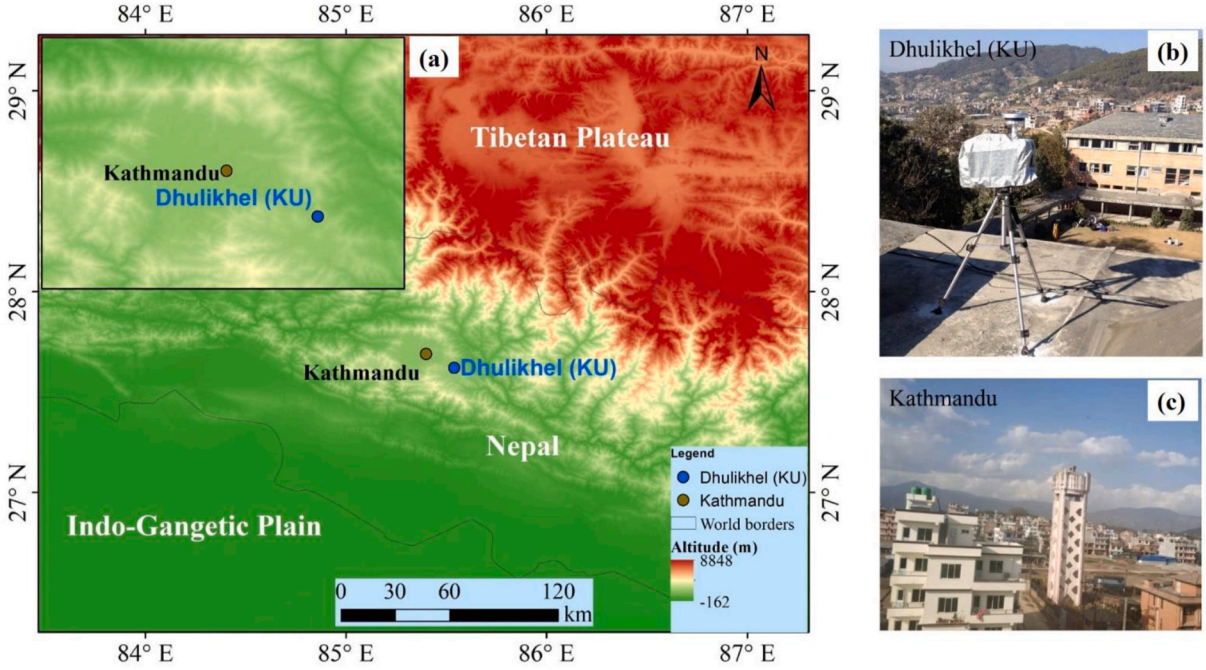

Fig. 1. The map of the study area with the sampling locations (Kathmandu and Dhulikhel) (a). Picture of sampling location at the rooftop of Library building, Dhulikhel (Kathmandu University) (b), and sampling location at Kathmandu Valley (c).

Qingdao Laoying, China) at a flow rate of 100 L min^{-1}. A $PM_{2.5}$ cyclone was used for $PM_{2.5}$. Details of the sampler and sampling methods have been described previously (Tripathee et al., 2021). The filters were exposed for 24 h and subsequently stored at −20 °C awaiting laboratory processing. The particulate mass was determined by gravimetric analysis using a microbalance (Mettler AE240, Mettler-Toledo Instruments Shanghai Co Ltd., China) with a sensitivity of ±0.01 mg.

2.3. Analytical, quality assurance, and quality control procedures

The total Hg concentration of the PM samples was examined following the United States Environmental Protection Agency (US EPA) Method 7473 on a direct mercury analyzer (Hydra-C type; Leeman Lab Hydra, Teledyne Leeman Laboratories, Hudson, NH, USA; Guo et al., 2017, 2020). Complete details of the laboratory methods, quality assurance, and quality control procedures for HgP analysis are presented in Text S1 in the Supplementary Material. The processing and analysis of the Hg isotopic composition of the sampled PM were conducted as described by Fu et al. (2019a). In brief, the reference material NIST-2711 (contaminated soil from Montana, USA) and Hg from the PM samples was pre-concentrated with 5 mL of a 40% mixed acid solution (v/v, $2HNO_3$/1HCl) using the double-stage combustion protocol described by Huang et al. (2015). The combustion of NIST-2711 yielded a mean recovery rate of 98.8 ± 8.6% ($n = 4$).

The isotopic compositions of Hg in the PM samples were determined using a Nu-plasma multi-collector inductively coupled plasma mass spectrometer (Nu Plasma II, Nu Instruments Ltd., UK) at the State Key Laboratory of Environmental Geochemistry of the Institute of Geochemistry at the Chinese Academy of Sciences. The MDF signatures of the HgP isotopes are reported in delta notation (e.g., δ^{202}Hg signatures) per mil (‰) with the NIST-3133 standard reference in brackets (Blum and Bergquist, 2007). The MIF signatures (e.g., Δ^{199}Hg, Δ^{200}Hg, and Δ^{201}Hg signatures) are reported as the deviation of the MDF signatures measured from the theoretically predicted signatures according to the kinetic MDF law (Blum and Bergquist, 2007).

We determined the analytical uncertainty of the HgP isotopic compositions during instrumental procedures by repeatedly analyzing the isotopic compositions of the NIST-3177 reference material. Regarding the δ^{202}Hg, Δ^{199}Hg, Δ^{200}Hg, and Δ^{201}Hg values, the means ± 2 standard deviations (SDs) were 0.52 ± 0.08‰, 0.00 ± 0.07‰, 0.00 ± 0.06‰, and −0.03 ± 0.09‰, respectively ($n = 9$). The δ^{202}Hg, Δ^{199}Hg, Δ^{200}Hg, and Δ^{201}Hg values of the reference material NIST-2711 were determined through the same method to be −0.23 ± 0.08‰, −0.19 ± 0.06‰, 0.01 ± 0.07‰, and −0.18 ± 0.06‰, respectively ($n = 4$). Overall, these results are consistent with those of previous studies (Blum and Johnson, 2017; Fu et al., 2019a). In the present study, we reported the analytical uncertainty (to 2 SDs) of the isotopic HgP compositions as the 2-SD results obtained through the repeated analysis of the NIST-3177 reference material, unless the uncertainty (within 2 SDs) of the repeated analysis of the same sample was larger than that of NIST-3177.

The OC and EC values were measured using a Sunset Carbon Analyzer (Atmoslytic Inc., Calabasas, CA, USA) according to the IMPROVE_A temperature protocol for thermal/optical carbon analysis (Chow et al., 2001). The acceptable variations in the replicated sample measurements were <3%. For OC, EC, and total carbon (TC), the detection limits were 0.41 μg cm^{-2}, 0.13 μg cm^{-2}, and 0.46 μg cm^{-2}, respectively.

2.4. Wind circulation and concentration-weighted trajectories

ERA-Interim is a global atmospheric reanalysis dataset collected by the European Centre for Medium-Range Weather Forecasts. Using the grid analysis and display system, maps of the horizontal wind circulation across Nepal were constructed from ERA-Interim monthly data of zonal and meridional winds from March to May 2018 (Figure S1). Furthermore, concentration-weighted trajectory (CWT) maps of the seasonal mass concentrations of HgP (pg m^{-3}) were produced to trace the potential source regions (Text S2, Figures S1 and S2).

3. Results and discussion

3.1. HgP concentrations in the Himalayan foothills

The results showed that HgP levels varied widely both in Dhulikhel (5.1–370 pg m^{-3}) and Kathmandu (234.5–1077.8 pg m^{-3}). The general statistics are presented in Table 1. The mean (±SD) HgP concentration in Dhulikhel was low (108.7 ± 86.2 pg m^{-3}; Table 1) compared with that of most cities in neighboring countries, such as Lhasa in China (224 ± 139 pg m^{-3}; Huang et al., 2016) and Mahasar in India (756.7 ± 436.3 pg m^{-3}; Kumari and Kulshrestha, 2018). The mean HgP concentration in Dhulikhel was similar to that reported for Seoul in South Korea (65.4 ± 47.8 pg m^{-3}; Nguyen et al., 2016), Zabrze in Poland (65.5 ± 53.7 pg m^{-3}; Pyta and Rogula-Kozłowska, 2016), and Tokyo in Japan (98 ± 51 pg m^{-3}; Sakata and Marumoto, 2002), whereas it was higher than that reported for Chicago in the USA (9 ± 20 pg m^{-3}; Gratz et al., 2013) and Göteborg in Sweden, (12.5 ± 5.9 pg m^{-3}; Li et al., 2008) (Fig. 2). In contrast, some of the highest HgP concentrations among nearby cities in South Asia were observed in the Kathmandu Valley (1982.8 ± 938.2 pg m^{-3}) during the pre-monsoon season (Table 1). These concentrations exceeded those measured in Chinese megacities such as Nanjing (1100 ± 570 pg m^{-3}; Zhu et al., 2014) and Beijing (573 ± 551 pg m^{-3}; Schleicher et al., 2015), as well as that in Mahasar, a rural area near New Delhi in India (756.7 ± 436.3 pg m^{-3}; Kumari and Kulshrestha, 2018). Moreover, our results from the same sampling days ($n = 13$) revealed that the Kathmandu Valley had significantly higher concentrations of TSP ($T = 237$; $n_1 = n_2 = 13$; $p < 0.05$) and HgP ($T = 260$; $n_1 = n_2 = 13$; $p < 0.05$) than Dhulikhel during the pre-monsoon season. Furthermore, the mean annual HgP concentration in Dhulikhel (108.89 ± 86.98 pg m^{-3}) was almost 7 times lower than the mean Hg-$PM_{2.5}$ concentration (742.1 ± 304.5 pg m^{-3}) and 18 times lower than the mean HgTSP concentration (1982.8 ± 938.2 pg m^{-3}) during the pre-monsoon season in the Kathmandu Valley (Fig. 2).

The HgP concentrations in the pre-monsoon season in the Kathmandu Valley are comparable to those obtained by other researchers over the same period (1855.4 ± 780.8 pg m^{-3}), but twice the mean concentration for 2013 and 2014 (850.5 ± 926.8 pg m^{-3}) (Guo et al., 2017). Local anthropogenic sources, such as soil particles and fuel combustion, could largely explain the high TSP and HgP concentrations in Kathmandu, as indicated by Guo et al. (2017). The Hg contained in soil particles originates partly from air deposition and natural sources in the valley. Relevant studies have reported that coal burning is the primary source of atmospheric Hg in Asia (Fang et al., 2009; Fu et al., 2011), thus supporting the present findings.

3.2. Seasonality and potential transport processes

Clear seasonal variations in HgP and TSP concentrations were observed during the study period. Although the mean HgP concentration for the pre-monsoon period (278.7 ± 91.9 pg m^{-3}) in Dhulikhel was considerably higher than the mean annual HgP concentration (108.9 ± 86.2 pg m^{-3}), it was very low compared with the corresponding concentration in the Kathmandu Valley over the same period (Figs. 2 and 3). As shown in Fig. 3, TSP mass ratios were lower during the monsoon season, primarily as a result of precipitation washout. Guo et al. (2020) also found that precipitation washout contributed significantly to reducing atmospheric HgP concentrations in Kanpur, an Indian metropolis in the central part of the IGP. The CWT of HgP suggests that areas in West Asia and the Arabian Desert were the main sources of HgP, thus explaining the high HgP concentrations in Dhulikhel during the pre-monsoon season (Figure S2). The transmission of aerosols from the IGP region also influenced Dhulikhel during the dry season, which is consistent with related research (Tripathee et al., 2021). Furthermore,

Table 1
Concentrations of TSP mass (μg m^{-3}), HgP (pg m^{-3}) with standard deviation and range (in brackets), and HgP/TSP (ng g^{-1}) in Dhulikhel (rural) and Kathmandu (urban) sites in different seasons.

Site/Classification (sample size)	Period (Season) (Cutoff-size)	TSP mass (±SD) (Range)	HgP concentration (±SD) (Range)	HgP/TSP[a] (Range)
Dhulikhel/Rural ($n = 72$)	Jan–Dec 2018 (Annual) (TSP)	229.1 (±108.2) (38–442.5)	108.9 (±86.2) (5.1–370)	427.72 (±241.1) (71.6–1193.9)
Dhulikhel/Rural ($n = 30$)	Mar–May 2018 (Pre-monsoon) (TSP	278.7 (±91.9) (74.1–442.5)	144.3 (±74.2) 29.5–331.7)	517.8 (±233.3) 238.7–1193.9)
Kathmandu/Urban ($n = 24$)	Mar–May 2018 (Pre-monsoon) (TSP)	588.7 (±237.8) (234.5–1077.8)	1982.8 (±938.2) (415.5–3545.3)	3545.2 (±1062.3) (997.1–5391.4)
Kathmandu/Urban ($n = 24$)	Mar–May 2018 (Pre-monsoon) ($PM_{2.5}$)	129.8 (±43.7) (76.2–238.6)	742.1 (±304.5) (256.3–1242.3)	5749.9 (±1778.1) (2649.8–9070.9)

[a] $PM_{2.5}$ samples was also analyzed in the Kathmandu Valley during pre-monsoon and is presented in the last row.

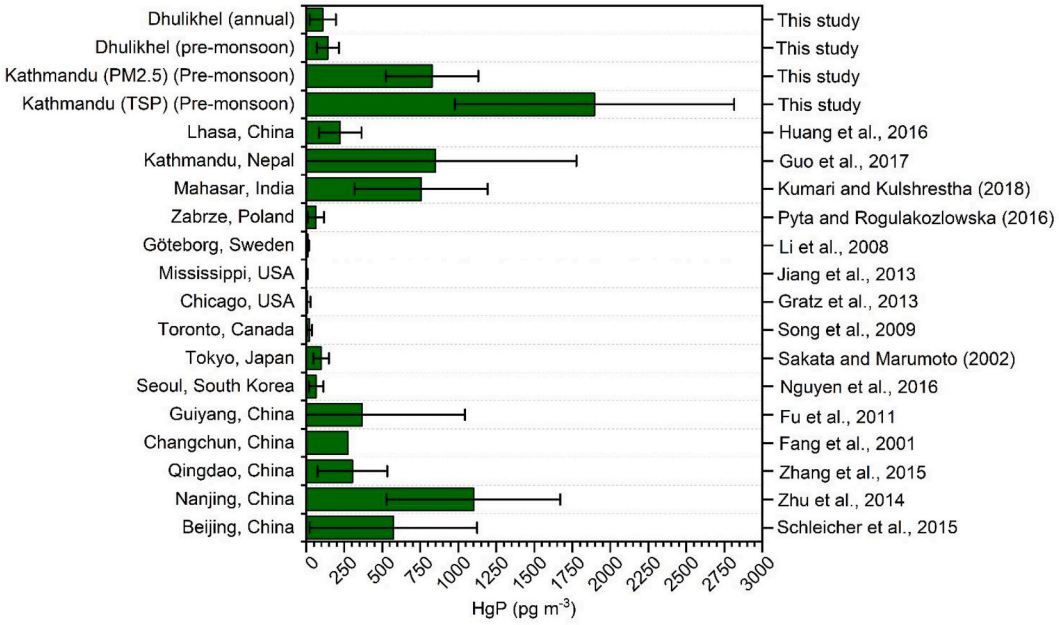

Fig. 2. Comparison of HgP (pg m^{-3}) in the present study with other major cities around the world.

weak-to-moderate source contributions from the west (e.g., the Kathmandu Valley) during the pre-monsoon season were found to contribute to the higher HgP concentrations in Dhulikhel (Figure S1). Dhulikhel is affected by air masses transported from the Bay of Bengal, whereby heavy rain occurs during the monsoon season (Figure S2), reducing pollutant concentrations. During dry periods, high atmospheric HgP concentrations and high aerosol mass may relate to high anthropogenic emissions (e.g., from transport) but low scavenging and deposition rates over the Himalayan foothills.

3.3. Affinity of HgP for carbon and the role of local transport

To identify their relationship with atmospheric HgP, the OC and EC concentrations in the TSP samples from Dhulikhel were measured. The HgP concentration was significantly positively correlated with OC, EC, and TC during the pre-monsoon, monsoon, and post-monsoon seasons ($p < 0.05$), but not with EC in winter (Figure S3). This implies the positive affinity of HgP for OC (and thus TC) in atmospheric particles throughout the year (Figure S4). This result also suggests that the sources of HgP (e.g., fossil fuel combustion and industry) are similar to those of carbonaceous particles. Parallel sampling of OC and EC during the pre-monsoon season ($n = 13$) at the two sites revealed the concentrations of OC-TSP ($T = 229$; $n_1 = n_2 = 13$; $p < 0.05$) and EC-TSP ($T = 252$; $n_1 = n_2 = 13$; $p < 0.05$) in the Kathmandu Valley were significantly higher than those in Dhulikhel. The low and relatively similar OC/EC ratios in Kathmandu (3.28 ± 1.02) and Dhulikhel (3.4 ± 1.24; Figure S5) suggest a similar source of carbonaceous aerosols, particularly fossil fuel combustion (Chen et al., 2020). This result also supports the hypothesis that Hg has a higher affinity for carbon, especially OC (Han et al., 2018; Yuan et al., 2020); however, the effects on HgP may vary depending on the carbonaceous particles involved (Duan et al., 2016). This further supports the possibility that winds from the Kathmandu Valley play a pivotal role in Hg pollution in Dhulikhel. The significant correlations between TSP mass ratios and HgP (Fig. 4a and b) and TC, EC, and OC (Fig. 4c and d) concentrations during the same sampling days at Dhulikhel and Kathmandu also indicate the local transport of these pollutants to Dhulikhel during this period (Fig. 4).

3.4. Hg content and non-isotopic source apportionment

The Hg content (HgP/TSP ratio) is useful for assessing the sources and enrichment of Hg, especially if the Hg concentrations of natural and anthropogenic components (e.g., soil and coal) in the region are available (Guo et al., 2020). The HgP/TSP ratio in Dhulikhel ranged from 72 ng g^{-1} to 1194 ng g^{-1} (mean of 428 ± 244 ng g^{-1}). The HgP/TSP and HgP/$PM_{2.5}$ ratios in the Kathmandu Valley ranged from 997 ng g^{-1} to 5391 ng g^{-1} (mean of 3545 ± 1062 ng g^{-1}) and from 2679 ng g^{-1} to 9070 ng g^{-1} (mean of 5750 ± 1778 ng g^{-1}), respectively, during the pre-monsoon season, suggesting a higher Hg content in fine particles. According to Feddersen et al. (2012), fine particles are mostly produced

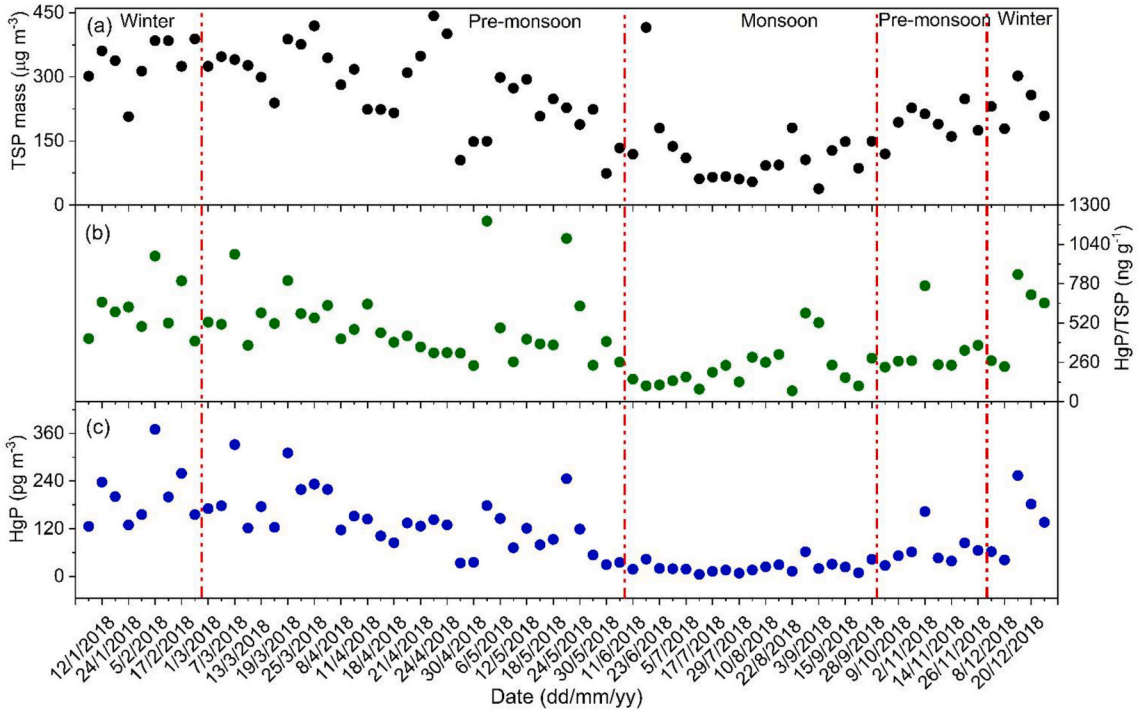

Fig. 3. Seasonal concentrations of (a) TSP mass (μg m^{-3}), (b) HgP/TSP (ng g^{-1}), and (c) HgP (pg m^{-3}) in Dhulikhel in 2018.

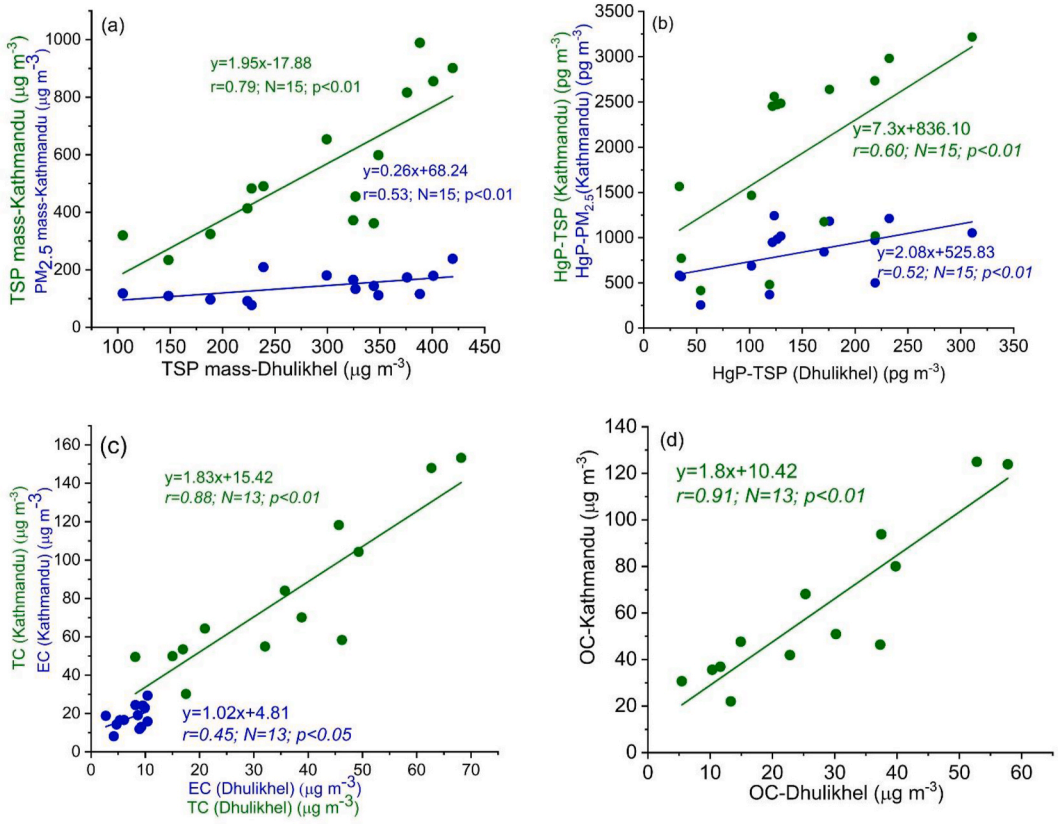

Fig. 4. Regression between TSP-mass in Dhulikhel with TSP-mass and $PM_{2.5}$ in Kathmandu (a); regression between HgP-TSP in Dhulikhel with HgP-TSP and HgP-$PM_{2.5}$ in Kathmandu (b); regression between EC in Dhulikhel/TC in Kathmandu with TC/EC in Kathmandu (c); and regression between OC in Dhulikhel with OC in Kathmandu (d); during pre-monsoon.

from fine crustal dust as well as organic and soot particles in continental locations. The fine particle concentrations in the study region are high during the pre-monsoon season because of increased anthropogenic emissions and the long-range transport of westerly air masses (Tripathee et al., 2017). The scavenging of Hg by small particles is higher than that of coarse particles, which is expected to result in a higher Hg content in fine particles. Another reason is the larger surface area of fine particles compared with coarse particles, which facilitates the adsorption of Hg (Li et al., 2017; Bo et al., 2016). In general, the mean HgP/TSP ratios during the pre-monsoon season and on an annual basis are much lower in Dhulikhel than in Kathmandu. Furthermore, the atmospheric Hg concentration in Kathmandu in the present study was comparable to that reported by Guo et al. (2017). However, the fact that the Hg content of $PM_{2.5}$ (as HgP/$PM_{2.5}$) in Kathmandu during the pre-monsoon season was higher than that of TSP (Table 1) suggests that fine ambient air particles in the Kathmandu Valley contained a relatively high Hg concentration during the study period.

A comparison of the HgP/TSP ratio of natural sources (e.g., dust and topsoil; 56–300 ng g^{-1}; Schleicher et al., 2016) with the background concentrations in Himalayan topsoil (3.82–105.7 ng g^{-1}; Tripathee et al., 2019b) revealed that the HgP/TSP ratio in Dhulikhel was higher than that of natural sources. This implies that Hg pollution in this region is the product of a combination of anthropogenic and natural sources, such as dust. Koshle et al. (2008) reported that the Hg content of Indian coal ranged from 1800 ng g^{-1} to 6100 ng g^{-1}, while that of soil at various locations near a steel plant in Bhilai ranged from 3590 ng g^{-1} to 16,580 ng g^{-1}. Therefore, the Hg content of the aerosol samples from Dhulikhel was probably primarily of a natural origin and underwent atmospheric transport from the valley. However, aerosol samples from Kathmandu included a mixture of natural and anthropogenic sources, which were affected by emissions of Indian coal and traffic, especially in the case of fine particles. A large amount of low-grade Indian coal is used in the brick kilns near the sampling site in Kathmandu during dry periods (Tripathee et al., 2017). Moreover, the use of Indian fuel in vehicles has a substantial impact on Hg levels in aerosols. The sources and transport of HgP at the study sites are further discussed from an isotopic perspective in the following sections.

Supplementary Figure S6 (a, b) presents the correlations of HgP with the HgP/TSP ratio and TSP mass ratio in Dhulikhel. The TSP concentration was significantly positively correlated with the HgP/TSP ratio ($R^2 = 0.73$, $p < 0.01$, $N = 73$; Figure S1(a), and HgP concentrations were significantly positively correlated with TSP mass ratios ($R^2 = 0.58$, $p < 0.01$, $N = 73$; Figure S6(b). This implies that TSP (e.g., dust and other chemicals) contributed to the HgP concentration. Specifically, TSP and Hg may have had the same or similar origins. Alternatively, gaseous forms of Hg (e.g., GOM) could have adsorbed to existing atmospheric particles in the same air mass before arriving at the sampling site. A similar phenomenon was observed in a previous year-long analysis of atmospheric HgP in the Kathmandu Valley (Guo et al., 2017). Although the correlation between the HgP/TSP ratio and TSP mass ratio ($R^2 = 0.16$, $p < 0.05$, $N = 73$; Figure S6(c) in the present study was weak, it could indicate that both had some impact on the HgP concentration. Studies at other locations have also revealed that HgP is primarily associated with PM (e.g., dust) or other chemical particles that are likely formed through the adsorption of Hg^{2+} onto atmospheric particles (Guo et al., 2017; Huang et al., 2016, 2020b).

3.5. Stable HgP isotopes

3.5.1. Mass-dependent fractionation in aerosol samples

The PM samples in this study were generally characterized by negative δ^{202}Hg values ranging from −1.42‰ to 0.28‰ (mean ± 2 SDs = −0.82‰ ± 0.08‰, $n = 14$; Fig. 5, Table S1). However, these values tended toward the positive side of the plots compared with emissions from industry, traffic, and coal (Fig. 5), but were similar to those in soil samples from the southern Himalayan slopes (Huang et al., 2020b). Nevertheless, the slightly negative δ^{202}Hg values in HgP relative to those previously reported for soil samples from the Nepalese Himalayas indicate that the sources of Hg may be local. As found in multiple studies (Guo et al., 2017; Tripathee et al., 2017, 2019a), there are numerous local sources of Hg in the Kathmandu Valley. This might explain the more negative MDF signatures of Hg (δ^{202}Hg), as reported for urban industrial sites in Kolkata, India (Das et al., 2016). Considering that the δ^{202}Hg signature matched those reported by Huang et al. (2020a) for

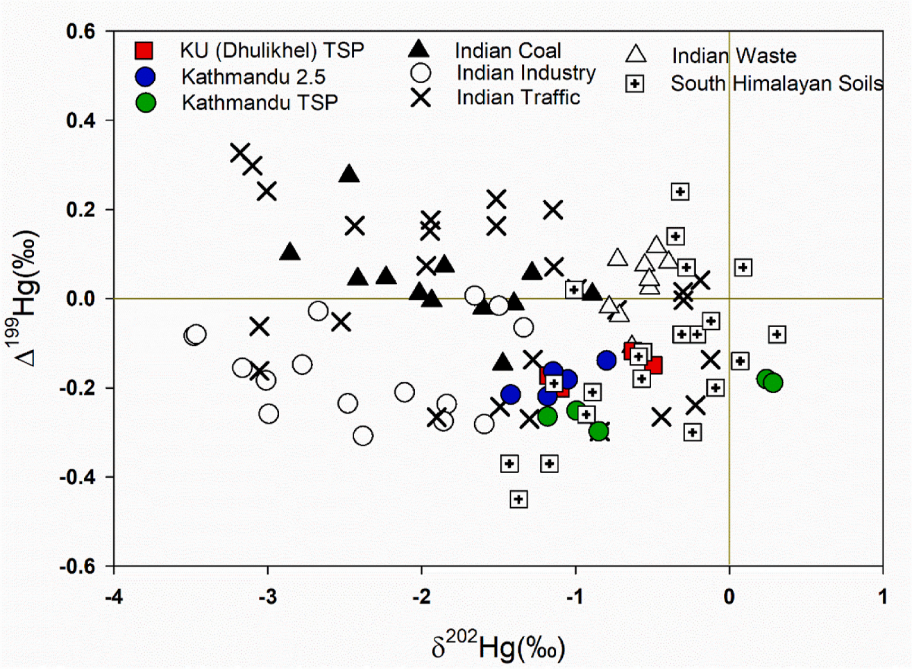

Fig. 5. Plot of Δ^{199}Hg (‰) versus δ^{202}Hg (‰) in the present study (Dhulikhel TSP, Kathmandu $PM_{2.5}$ and Kathmandu TSP). Also included in the plot are the data from nearby areas in Kolkata-India (Indian coal, Indian industry, Indian traffic and Indian wastes (Das et al., 2016), and South slope of the Himalayas (Huang et al., 2020a).

Himalayan lake sediments and Das et al. (2016) for Indian waste (biomass), the probable sources of Hg in the present study were soil erosion and waste burning. Furthermore, India releases a vast amount of Hg into the atmosphere via fossil fuel combustion (Burger Chakraborty et al., 2013) and waste biomass burning (Das et al., 2016), which can reach the Himalayas through long-range transport (Tripathee et al., 2021). Some of the HgP may also have been carried to the study area through air by the South Asian monsoon (Huang et al., 2020a, 2020b), given its long residence time (Das et al., 2016). This argument is supported by the fact that the positive δ^{202}Hg values in some samples were similar to those reported by Sun et al. (2016). In addition, the contribution of westerlies circulating through the IGP region to atmospheric HgP concentrations should not be disregarded, as indicated by the back trajectories during the pre-monsoon season (Figure S2).

The primary sources of atmospheric Hg in Asian countries have been determined to be anthropogenic, including cement production and coal combustion (Fang et al., 2009; Fu et al., 2011; Guo et al., 2020; Huang et al., 2016, 2017). Domestic emissions and long-range transport can also contribute to Hg pollution, depending on the location (Fu et al., 2019a). The high aerosol concentrations during the pre-monsoon season in the area surrounding the study region, which were obtained using an aerosol optical depth (AOD) at 0.55 μm (Figure S7), confirmed the contribution of regional transported dust and smoke (Tripathee et al., 2021). Cloud-Aerosol Lidar with Orthogonal Polarization (CALIOP) data during the pre-monsoon season also demonstrate that dust and smoke pollution could transport Hg particles regionally at elevations of 5–7 km (Figure S8). Overall, the AOD, CALIOP, and CWT data suggest that the study sites were impacted by the long-range regional transport of pollutants, which is consistent with our initial assumptions.

3.5.2. Mass independent fractionation in aerosol samples

Because the photoreduction of Hg(II) in aerosols produces negative values of Δ^{199}Hg and Δ^{201}Hg through the MIF of odd numbered Hg isotopes in natural samples (Sonke, 2011; Sun et al., 2016; Zerkle et al., 2020), Δ^{199}Hg signatures are also useful for identifying Hg contamination pathways. However, this is not the case in observations of wet atmospheric precipitation, which produces positive concentrations of oceanic Δ^{199}Hg and negative concentrations of atmospheric Δ^{199}Hg (Sonke, 2011). Terrestrial plants and soils, which primarily store Hg0, release less odd-mass-number isotopes of Hg; thus, negative MIFs are present in the retained fraction (Huang et al., 2016). In the present study, the proportion of Δ^{199}Hg in the measured HgP concentrations ranged from −0.30‰ to −0.12‰ (mean ± 2 SDs = −0.16‰ ± 0.07‰, n = 14; Table S1), which are within the range of (or less than) that in soil samples from the southern Himalayan slopes (Fig. 6; Huang et al., 2020a). Based on the indirect approach taken by Sonke (2011), this result indicates that local soils, under anthropogenic impacts, are a probable source of HgP in the Kathmandu Valley. This is supported by the fact that pollutants of anthropogenic origin are generally characterized by lower Δ^{199}Hg concentrations relative to the background atmospheric concentrations (Sun et al., 2016; Fu et al., 2019). Fig. 6 reveals the similarity between the present results for Hg-MIF and those in Indian industry (Das et al., 2016). Thus, the atmospheric HgP observed in the present study in the Kathmandu Valley could have primarily originated from nonintentional generation in byproduct sectors, such as the manufacturing of metal and cement, the combustion of coal and oil, and gold mining without Hg amalgamation (Das et al., 2016; Sun et al., 2016). The overlap between the range in which Δ^{199}Hg pollution was observed in the present study and in Indian traffic emissions should not be neglected as another potential source. Specifically, the considerable amount of vehicular emissions in the Kathmandu Valley likely contributes to HgP pollution. Therefore, the mixture of soil and anthropogenic sources of HgP pollution (e.g., Indian coal and industry) also potentially affects the corresponding HgP concentration in the Himalayan foothills.

3.6. Environmental implications

Numerous studies have documented the long-range transport and deposition of pollutants such as Hg to the Himalayas over the IGP via westerlies during the dry season and the Indian monsoon during the rainy season (Guo et al., 2017; Huang et al., 2020a,b). Under the impacts of local pollution from soil and fuel combustion, urban areas in South Asia, particularly those in the Himalayan foothills, have relatively high concentrations of atmospheric Hg (Guo et al., 2017, 2020). The present findings further support the hypothesis that high emissions of PM and

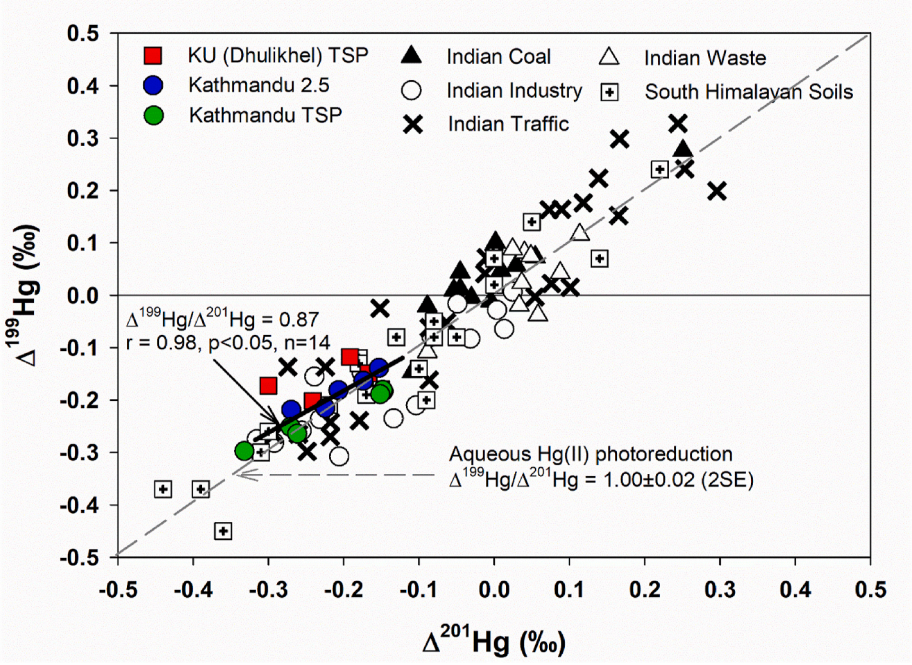

Fig. 6. Plot of Δ^{199}Hg (‰) versus Δ^{201}Hg (‰) in the present study (data sets are the same as in Fig. 5). The dashed grey line indicates a slope of 1.00 as of Aqueous Hg(II) photoreduction (Bergquist and Blum, 2007). The solid black line (short line) represents the data from the present study with a slope of 0.87.

Hg from anthropogenic activities contribute to elevated HgP concentrations in urban Himalayan areas. Furthermore, the atmospheric Hg that is released locally from urban areas in the Himalayan foothills (e.g., Kathmandu) may be transported downwind to relatively non-polluted areas such as Dhulikhel. Despite the ambiguity in the interpretation of data on the isotopic composition of HgP (Kwon et al., 2020), stable isotope analysis is becoming an essential tool in the apportionment of Hg sources. Its validity has been established through the application of new and advanced technologies (Yamakawa et al., 2020). The present study demonstrates that monitoring the regional and local dynamics of Hg pollution is vital for environmental management, despite the fact that Hg is a global pollutant that can be transported over long distances. Future research should focus on quantifying the source contribution of Hg according to local, regional, and long-range transport patterns.

4. Conclusions

This study examined the sources of atmospheric HgP on the basis of isotopic signatures of Hg in samples obtained from Kathmandu and Dhulikhel, which are areas in the Himalayan foothills with high and low anthropogenic pressures, respectively. The TSP mass ratio and HgP concentration in the Kathmandu Valley were higher than those in Dhulikhel. Both isotopic (δ^{200}Hg and Δ^{199}Hg) and non-isotopic evidence indicated that dust from soil erosion and smoke from the burning of biomass (including waste), as well as nonintentional generation from industrial byproducts (without Hg amalgamation) were the major sources of Hg in Kathmandu. Long-range transport from the IGP and dust resuspension by local anthropogenic activities could have contributed to the observed Hg pollution. The hypothesis that Hg is transported from Kathmandu to Dhulikhel via short-range transport was supported by the OC/EC ratio and seasonal trends of the TSP mass ratio and HgP concentration. Therefore, the resuspension of already deposited Hg may constitute a major source of atmospheric Hg pollution in anthropogenically disturbed areas. Thus, the mechanisms underlying local, regional, and long-range transport should be considered in the examination of atmospheric Hg pollution.

Declaration of competing interest

The authors declare that they have no known competing financial interests or personal relationships that could have appeared to influence the work reported in this paper.

Acknowledgments

This work was supported by the National Natural Science Foundation of China (41801042, 41630754), the Second Tibetan Plateau Scientific Expedition and Research Program (2019QZKK0605), the Pan-Third Pole Environment Study for a Green Silk Road (XDA20040501), the Chinese Academy of Sciences “Light of West China” program, and the State Key Laboratory of Cryospheric Science (SKLCS-ZZ-2020). The Chinese Academy of Sciences has supported Dr. Lekhendra Tripathee (corresponding author) under the President’s International Fellowship Initiative (2020FYC0001) and Chhatra Mani Sharma (coauthor) as Visiting Scientist. This study is part of a framework within the Atmospheric Pollution and Cryospheric Change (APCC) observation network. The authors thank Dr. Maheswar Rupakheti from the Institute for Advanced Sustainability Studies for providing space and Mr. Shyam Kumar Newar for sampling at the Kathmandu site.

Appendix A. Supplementary data

Supplementary data to this article can be found online at https://doi.org/10.1016/j.envpol.2021.117317.

Author contributions statement

Junming Guo: Writing orignal Draft, Investigation, Project administration. Chhatra Mani Sharma: Investigation, Field support, Writing – review & editing, Lekhendra Tripathee: Conceptualization, Investigation, Methodology, Writing – review & editing. Shichang Kang: Supervision, Resources, Writing – review & editing. Xuewu Fu: Methodology, Writing – review & editing Jie Huang: Investigation, Writing – review & editing. Kundan Lal Shrestha: Aerosol sampling, Writing – review & editing. Pengfei Chen: Data curation, Writing – review & editing.

References

Bergquist, B.A., Blum, J.D., 2007. Mass-dependent and -independent fractionation of Hg isotopes by photoreduction in aquatic systems. Science 318, 417. https://doi.org/10.1126/science.1148050.

Blum, J.D., Johnson, M.W., 2017. Recent developments in mercury stable isotope analysis. Rev. Mineral. Geochem. 82, 733–757. https://doi.org/10.2138/rmg.2017.82.17.

Blum, J.D., Sherman, L.S., Johnson, M.W., 2014. Mercury isotopes in earth and environmental sciences. Annu. Rev. Earth Planet Sci. 42, 249–269. https://doi.org/10.1146/annurev-earth-050212-124107.

Bo, D., Cheng, J., Xie, H., Zhao, W., Wei, Y., Chen, X., 2016. Mercury concentration in fine atmospheric particles during haze and non-haze days in Shanghai, China. Atmos. Pollut. Res. 7, 348–354. https://doi.org/10.1016/j.apr.2015.10.002.

Burger Chakraborty, L., Qureshi, A., Vadenbo, C., Hellweg, S., 2013. Anthropogenic mercury flows in India and impacts of emission controls. Environ. Sci. Technol. 47, 8105–8113. https://doi.org/10.1021/es401006k.

Chen, P., Kang, S., Tripathee, L., Ram, K., Rupakheti, M., Panday, A.K., Zhang, Q., Guo, J., Wang, X., Pu, T., Li, C., 2020. Light absorption properties of elemental carbon (EC) and water-soluble brown carbon (WS–BrC) in the Kathmandu Valley, Nepal: a 5-year study. Environ. Pollut. 261, 114239.

Cheng, N., Duan, L., Xiu, G., Zhao, M., Qian, G., 2017. Comparison of atmospheric PM2.5-bounded mercury species and their correlation with bromine and iodine at coastal urban and island sites in the eastern China. Atmos. Res. 183, 17–25. https://doi.org/10.1016/j.atmosres.2016.08.009.

Chow, J.C., Watson, J.G., Crow, D., Lowenthal, D.H., Merrifield, T., 2001. Comparison of IMPROVE and NIOSH carbon measurements. Aerosol Sci. Technol. 34, 23–34. https://doi.org/10.1080/02786820119073.

Das, R., Wang, X., Khezri, B., Webster, R.D., Sikdar, P.K., Datta, S., 2016. Mercury isotopes of atmospheric particle bound mercury for source apportionment study in urban Kolkata, India. Elem. Sci. Anthr. 4, 000098 https://doi.org/10.12952/journal.elementa.000098.

Duan, L., Xiu, G., Feng, L., Cheng, N., Wang, C., 2016. The mercury species and their association with carbonaceous compositions, bromine and iodine in PM2.5 in Shanghai. Chemosphere 146, 263–271. https://doi.org/10.1016/j.chemosphere.2015.11.058.

Fang, G.-C., Lin, Y.-H., Zheng, Y.-C., 2016. Ambient air particulates and particulate-bound mercury Hg(p) concentrations: dry deposition study over a Traffic, Airport, Park (T.A.P.) areas during years of 2011–2012. Environ. Geochem. Health 38, 183–194. https://doi.org/10.1007/s10653-015-9702-3.

Fang, G.-C., Wu, Y.-S., Chang, T.-H., 2009. Comparison of atmospheric mercury (Hg) among Korea, Japan, China and Taiwan during 2000–2008. J. Hazard Mater. 162, 607–615. https://doi.org/10.1016/j.jhazmat.2008.05.142.

Feddersen, D.M., Talbot, R., Mao, H., Sive, B.C., 2012. Size distribution of particulate mercury in marine and coastal atmospheres. Atmos. Chem. Phys. 12, 10899–10909. https://doi.org/10.5194/acp-12-10899-2012.

Fu, X., Feng, X., Qiu, G., Shang, L., Zhang, H., 2011. Speciated atmospheric mercury and its potential source in Guiyang, China. Atmos. Environ. Times 45, 4205–4212. https://doi.org/10.1016/j.atmosenv.2011.05.012.

Fu, X., Zhang, H., Feng, X., Tan, Q., Ming, L., Liu, C., Zhang, L., 2019a. Domestic and transboundary sources of atmospheric particulate bound mercury in remote areas of China: evidence from mercury isotopes. Environ. Sci. Technol. 53, 1947–1957. https://doi.org/10.1021/acs.est.8b06736.

Fu, X., Zhang, H., Liu, C., Zhang, H., Lin, C.-J., Feng, X., 2019b. Significant seasonal variations in isotopic composition of atmospheric total gaseous mercury at forest sites in China caused by vegetation and mercury sources. Environ. Sci. Technol. 53, 13748–13756. https://doi.org/10.1021/acs.est.9b05016.

Gratz, L.E., Keeler, G.J., Marsik, F.J., Barres, J.A., Dvonch, J.T., 2013. Atmospheric transport of speciated mercury across southern Lake Michigan: influence from emission sources in the Chicago/Gary urban area. Sci. Total Environ. 448, 84–95. https://doi.org/10.1016/j.scitotenv.2012.08.076.

Guo, J., Kang, S., Huang, J., Zhang, Q., Rupakheti, M., Sun, S., Tripathee, L., Rupakheti, D., Panday, A.K., Sillanpää, M., Paudyal, R., 2017. Characterizations of atmospheric particulate-bound mercury in the Kathmandu Valley of Nepal, South Asia. Sci. Total Environ. 579, 1240–1248. https://doi.org/10.1016/j.scitotenv.2016.11.110.

Guo, J., Ram, K., Tripathee, L., Kang, S., Huang, J., Chen, P., Ghimire, P.S., 2020. Study on mercury in PM_{10} at an urban site in the central Indo-Gangetic Plain: seasonal variability and influencing factors. Aerosol Air Qual. Res. 20, 2729–2740. https://doi.org/10.4209/aaqr.2019.12.0630.

Han, D., Zhang, J., Hu, Z., Ma, Y., Duan, Y., Han, Y., Chen, X., Zhou, Y., Cheng, J., Wang, W., 2018. Particulate mercury in ambient air in Shanghai, China: size-specific distribution, gas–particle partitioning, and association with carbonaceous composition. Environ. Pollut. 238, 543–553. https://doi.org/10.1016/j.envpol.2018.03.088.

Huang, J., Kang, S., Guo, J., Zhang, Q., Cong, Z., Sillanpää, M., Zhang, G., Sun, S., Tripathee, L., 2016. Atmospheric particulate mercury in Lhasa city, Tibetan Plateau. Atmos. Environ. 142, 433–441. https://doi.org/10.1016/j.atmosenv.2016.08.021.

Huang, J., Kang, S., Yin, R., Guo, J., Lepak, R., Mika, S., Tripathee, L., Sun, S., 2020a. Mercury isotopes in frozen soils reveal transboundary atmospheric mercury deposition over the Himalayas and Tibetan Plateau. Environ. Pollut. 256, 113432. https://doi.org/10.1016/j.envpol.2019.113432.

Huang, J., Kang, S., Yin, R., Lin, M., Guo, J., Ram, K., Li, C., Sharma, C., Tripathee, L., Sun, S., Wang, F., 2020b. Decoupling natural and anthropogenic mercury and lead transport from south Asia to the Himalayas. Environ. Sci. Technol. 54, 5429–5436. https://doi.org/10.1021/acs.est.0c00429.

Huang, Q., Liu, Y., Chen, J., Feng, X., Huang, W., Yuan, S., Cai, H., Fu, X., 2015. An improved dual-stage protocol to pre-concentrate mercury from airborne particles for precise isotopic measurement. J. Anal. At. Spectr. 30, 957–966. https://doi.org/10.1039/C4JA00438H.

Huang, Y., Deng, M., Li, T., Japenga, J., Chen, Q., Yang, X., He, Z., 2017. Anthropogenic mercury emissions from 1980 to 2012 in China. Environ. Pollut. 226, 230–239. https://doi.org/10.1016/j.envpol.2017.03.059.

Kang, S., Zhang, Q., Qian, Y., Ji, Z., Li, C., Cong, Z., Zhang, Y., Guo, J., Du, W., Huang, J., You, Q., Panday, A.K., Rupakheti, M., Chen, D., Gustafsson, Ö., Thiemens, M.H., Qin, D., 2019. Linking atmospheric pollution to cryospheric change in the Third Pole region: current progress and future prospects. Natl. Sci. Rev. 6, 796–809. https://doi.org/10.1093/nsr/nwz031.

Kim, P.-R., Han, Y.-J., Holsen, T.M., Yi, S.-M., 2012. Atmospheric particulate mercury: concentrations and size distributions. Atmos. Environ. 61, 94–102. https://doi.org/10.1016/j.atmosenv.2012.07.014.

Koshle, A., Pervez, Y.F., Tiwari, R.P., Pervez, S., 2008. Environmental pathways and distribution pattern of total mercury among soils and groundwater matrices around an integrated steel plant in India. J. Sci. Ind. Res. 67, 523–530.

Kumari, A., Kulshrestha, U., 2018. Trace ambient levels of particulate mercury and its sources at a rural site near Delhi. J. Atmos. Chem. 75, 335–355. https://doi.org/10.1007/s10874-018-9377-0.

Kwon, S.Y., Blum, J.D., Yin, R., Tsui, M.T.-K., Yang, Y.H., Choi, J.W., 2020. Mercury stable isotopes for monitoring the effectiveness of the Minamata Convention on Mercury. Earth Sci. Rev. 203, 103111. https://doi.org/10.1016/j.earscirev.2020.103111.

Li, J., Sommar, J., Wangberg, I., Lindqvist, O., Wei, S., 2008. Short-time variation of mercury speciation in the urban of Göteborg during GÖTE-2005. Atmos. Environ. 42, 8382–8388. https://doi.org/10.1016/j.atmosenv.2008.08.007.

Li, Yaxin, Wang, Y., Li, Yan, Li, T., Mao, H., Talbot, R., Nie, X., Wu, C., Zhao, Y., Hou, C., Wang, G., Zhou, J., Qie, G., 2017. Characteristics and potential sources of atmospheric particulate mercury in Jinan, China. Sci. Total Environ. 574, 1424–1431. https://doi.org/10.1016/j.scitotenv.2016.08.069.

Lindberg, S., Bullock, R., Ebinghaus, R., Engstrom, D., Feng, X., Fitzgerald, W., Pirrone, N., Prestbo, E., Seigneur, C., 2007. A synthesis of progress and uncertainties in attributing the sources of mercury in deposition. AMBIO A J. Hum. Environ. 36, 19–33.

Mukherjee, A.B., Bhattacharya, P., Sarkar, A., Zevenhoven, R., 2009. Mercury emissions from industrial sources in India and its effects in the environment. In: Mason, R., Pirrone, N. (Eds.), Mercury Fate and Transport in the Global Atmosphere. Springer US, Boston, MA, pp. 81–112. https://doi.org/10.1007/978-0-387-93958-2_4.

Nguyen, D.L., Kim, J.Y., Shim, S.-G., Ghim, Y.S., Zhang, X.-S., 2016. Shipboard and ground measurements of atmospheric particulate mercury and total mercury in precipitation over the Yellow Sea region. Environ. Pollut. 219, 262–274. https://doi.org/10.1016/j.envpol.2016.10.020.

Obrist, D., Johnson, D.W., Lindberg, S.E., Luo, Y., Hararuk, O., Bracho, R., Battles, J.J., Dail, D.B., Edmonds, R.L., Monson, R.K., Ollinger, S.V., Pallardy, S.G., Pregitzer, K. S., Todd, D.E., 2011. Mercury distribution across 14 U.S. forests. part I: spatial patterns of concentrations in biomass, litter, and soils. Environ. Sci. Technol. 45, 3974–3981. https://doi.org/10.1021/es104384m.

Pyta, H., Rogula-Kozłowska, W., 2016. Determination of mercury in size-segregated ambient particulate matter using CVAAS. Microchem. J. 124, 76–81. https://doi.org/10.1016/j.microc.2015.08.001.

Qie, G., Wang, Y., Wu, C., Mao, H., Zhang, P., Li, T., Li, Y., Talbot, R., Hou, C., Yue, T., 2018. Distribution and sources of particulate mercury and other trace elements in PM2.5 and PM10 atop Mount Tai, China. J. Environ. Manag. 215, 195–205. https://doi.org/10.1016/j.jenvman.2018.03.050.

Sakata, M., Marumoto, K., 2002. Formation of atmospheric particulate mercury in the Tokyo metropolitan area. Atmos. Environ. 36, 239–246. https://doi.org/10.1016/S1352-2310(01)00432-0.

Schleicher, N.J., Schäfer, J., Blanc, G., Chen, Y., Chai, F., Cen, K., Norra, S., 2015. Atmospheric particulate mercury in the megacity Beijing: spatio-temporal variations and source apportionment. Atmos. Environ. 109, 251–261. https://doi.org/10.1016/j.atmosenv.2015.03.018.

Schleicher, N.J., Schäfer, J., Chen, Y., Blanc, G., Chen, Y., Chai, F., Cen, K., Norra, S., 2016. Atmospheric particulate mercury in the megacity Beijing: efficiency of mitigation measures and assessment of health effects. Atmos. Environ. 124, 396–403. https://doi.org/10.1016/j.atmosenv.2015.09.040.

Siudek, P., Frankowski, M., Siepak, J., 2016. Atmospheric particulate mercury at the urban and forest sites in central Poland. Environ. Sci. Pollut. Res. 23, 2341–2352. https://doi.org/10.1007/s11356-015-5476-5.

Song, X., Cheng, I., Lu, J., 2009. Annual atmospheric mercury species in Downtown Toronto, Canada. J. Environ. Monit. 11, 660–669. https://doi.org/10.1039/b815435j.

Sonke, J.E., 2011. A global model of mass independent mercury stable isotope fractionation. Geochem. Cosmochim. Acta 75, 4577–4590. https://doi.org/10.1016/j.gca.2011.05.027.

Sun, R., Streets, D.G., Horowitz, H.M., Amos, H.M., Liu, G., Perrot, V., Toutain, J.-P., Hintelmann, H., Sunderland, E.M., Sonke, J.E., 2016. Historical (1850–2010) mercury stable isotope inventory from anthropogenic sources to the atmosphere. Elem. Sci. Anthr. 4, 000091 https://doi.org/10.12952/journal.elementa.000091.

Tang, Y., Wang, S., Wu, Q., Liu, K., Li, Z., Zou, J., Hou, D., Wu, Y., Duan, L., 2019. Measurement of size-fractionated particulate-bound mercury in Beijing and implications on sources and dry deposition of mercury. Sci. Total Environ. 675, 176–183. https://doi.org/10.1016/j.scitotenv.2019.04.245.

Tripathee, L., Kang, S., Chen, P., Bhattarai, H., Guo, J., Shrestha, K.L., Sharma, C.M., Ghimire, P.S., Huang, J., 2021. Water-soluble organic and inorganic nitrogen in ambient aerosols over the Himalayan middle hills: seasonality, sources, and transport pathways. Atmos. Res. 250, 105376. https://doi.org/10.1016/j.atmosres.2020.105376.

Tripathee, L., Guo, J., Kang, S., Paudyal, R., Huang, J., Sharma, C.M., Zhang, Q., Chen, P., Ghimire, P.S., Sigdel, M., 2019a. Spatial and temporal distribution of total mercury in atmospheric wet precipitation at four sites from the Nepal-Himalayas. Sci. Total Environ. 655, 1207–1217. https://doi.org/10.1016/j.scitotenv.2018.11.338.

Tripathee, L., Guo, J., Kang, S., Paudyal, R., Huang, J., Sharma, C.M., Zhang, Q., Rupakheti, D., Chen, P., Sharma Ghimire, P., Gyawali, A., 2019b. Concentration and risk assessments of mercury along the elevation gradient in soils of Langtang Himalayas, Nepal. Hum. Ecol. Risk Assess. 25, 1006–1017. https://doi.org/10.1080/10807039.2018.1459180.

Tripathee, L., Kang, S., Rupakheti, D., Cong, Z., Zhang, Q., Huang, J., 2017. Chemical characteristics of soluble aerosols over the central Himalayas: insights into spatiotemporal variations and sources. Environ. Sci. Pollut. Res. 24, 24454–24472. https://doi.org/10.1007/s11356-017-0077-0.

Xu, L., Chen, J., Yang, L., Niu, Z., Tong, L., Yin, L., Chen, Y., 2015. Characteristics and sources of atmospheric mercury speciation in a coastal city, Xiamen, China. Chemosphere 119, 530–539. https://doi.org/10.1016/j.chemosphere.2014.07.024.

Yamakawa, A., Bérail, S., Amouroux, D., Tessier, E., Barre, J., Sano, T., Nagano, K., Kanwal, S., Yoshinaga, J., Donard, O.F.X., 2020. Hg isotopic composition and total Hg mass fraction in NIES Certified Reference Material No. 28 Urban Aerosols. Anal. Bioanal. Chem. 412, 4483–4493. https://doi.org/10.1007/s00216-020-02691-9.

Yu, B., Fu, X., Yin, R., Zhang, H., Wang, X., Lin, C.-J., Wu, C., Zhang, Y., He, N., Fu, P., Wang, Z., Shang, L., Sommar, J., Sonke, J.E., Maurice, L., Guinot, B., Feng, X., 2016. Isotopic composition of atmospheric mercury in China: new evidence for sources and transformation processes in air and in vegetation. Environ. Sci. Technol. 50, 9262–9269. https://doi.org/10.1021/acs.est.6b01782.

Yuan, W., Wang, X., Lin, C.-J., Wu, C., Zhang, L., Wang, B., Sommar, J., Lu, Z., Feng, X., 2020. Stable mercury isotope transition during postdepositional decomposition of biomass in a forest ecosystem over five centuries. Environ. Sci. Technol. 54 (14), 8739–8749. https://doi.org/10.1021/acs.est.0c00950.

Zerkle, A.L., Yin, R., Chen, C., Li, X., Izon, G.J., Grasby, S.E., 2020. Anomalous fractionation of mercury isotopes in the Late Archean atmosphere. Nat. Commun. 11, 1709. https://doi.org/10.1038/s41467-020-15495-3.

Zhu, J., Wang, T., Talbot, R., Mao, H., Yang, X., Fu, C., Sun, J., Zhuang, B., Li, S., Han, Y., Xie, M., 2014. Characteristics of atmospheric mercury deposition and size-fractionated particulate mercury in urban Nanjing, China. Atmos. Chem. Phys. 14, 2233–2244. https://doi.org/10.5194/acp-14-2233-2014.